Dynamic behaviour of two stages planetary gearbox in non-stationary operations

Ahmed Hammami[1,2], Alfonso Fernandez Del Rincon[2], Fernando Viadero Rueda[2], Fakher Chaari[1], Mohamed Haddar[1]

[1] Dynamics of Mechanical Systems Research Unit- National School of Engineers Sfax
BP 1173 – 3038 – Sfax – Tunisia
[2] Department of Structural and Mechanical Engineering - Faculty of Industrial and Telecommunications Engineering - University of Cantabria - Avda. de los Castros s/n - 39005 Santander- Spain.
ahmed_hammami@voila.fr, alfonso.fernandez@unican.es, fernando.viadero@unican.es, fakher.chaari@gmail.com, mohamed.haddar@enis.rnu.tn

Abstract:

Planetary gears operate frequently in non stationary conditions. In this paper, variable load and run up are the non stationary excitations for back to back planetary gearboxes. In order to understand the dynamic behaviour of back to back planetary gears, a mathematical model is developed in stationary conditions. A variable load for an enslavement system is included in the model. Using the Short Time Fourier Transform, an amplitude-frequency modulation is observed on the run up. An extensive experimental study on the back to back planetary gear test rig was achieved in order to validate numerical results.
Keywords back to back planetary gear, non stationary condition, variable load, run up, dynamic behaviour

1. Introduction

Gears are excellent mechanisms for power transmission seen their high efficiency and load capacity uses and works to which they are devoted. Planetary gears are particularly useful for transmitting significant power with large speed reductions or multiplications. These kinds of gears are used in many fields of application like wind turbines, new generation aircraft engines, hybrid car transmissions etc…

Research developments in planetary gears become a necessity in order to improve efficiency and compactness and to decrease noise and price. Most studies were devoted to stationary condition where loads and speeds are constants. However, repetitive run up, time varying loading and speed conditions are very common in many industrial applications of planetary gears which imply non stationary operations. If we add excessive applied torque, manufacturing or installation errors, the transmission will be subjected to instability and severe vibrations.

Hidaka [8] studied the load sharing behaviour of planetary gear set. Kahraman [9] developed a model to predict load sharing of planets under quasi-static conditions. Ligata [10] investigated the influence of several system level factors in gear stress. Inalpolat [11] presented a theoretical and experimental investigation on modulation sidebands observed in planetary gear.

For the non stationary operations, the speed's fluctuation will modify the structure of the frequency response: Randal [1] justified that the vibration amplitude which is induced by meshing process is modulated by load fluctuation. Bartelmus [2] found that the shape of the transmission error function changes as a result of load variation. Chaari [3-4-5] studied the influence of local damage and time varying load on the vibration response and highlighted by a model based approach, the amplitude and frequency modulations accruing for non stationary operating conditions. Kim [6] studied the dynamic behaviour of a planetary gear when component gears have time-varying pressure angles and contact ratios. Khabou [7] studied the dynamic behaviour of a spur gear in transient regime. The spur gear is driven firstly by an electric motor and than by four strokes four cylinders diesel engine.

Many other authors were interested in dynamics of multiple stages or compound planetary gearboxes. Ligata [15] presented an experimental study to describe the impact of certain types of manufacturing errors on gear stresses and the individual planets loads of n planets planetary gear set (n=3-6) on back to back planetary gear. Singh [16] presented an experimental and theoretical study in order to determine the influence of certain key factor in planetary transmissions on gear stresses and planetary load sharing on multi-stage planetary gear.

In this paper, we are interested in the characterization of two stage planetary gears mounted back to back. First, a mathematic model is developed. Variable load and run up effects are modelled. Simulation of the dynamic behaviour of this transmission is presented highlighting the non stationary effects. Finally, correlations between numerical and experimental results are presented.

2. Numerical model

The model of back to back planetary gear is a torsional model based on that of Lin and Parker [12]. The components are the ring (r), the sun (s), planets (1, 2, 3) and carrier (c) which carries the planets in the reaction gear set and in the test gear set as shown in Fig.1.

The test ring and the test sun are respectively linked to the three planets of the test gear set via teeth mesh stiffness K_{rt1}, K_{rt2}, K_{rt3} and K_{st1}, K_{st2}, K_{st3}. The same is on the reaction gear set, the reaction ring and the reaction sun are respectively linked to the three planets via teeth mesh stiffness K_{rr1}, K_{rr2}, K_{rr3} and K_{sr1}, K_{sr2}, K_{sr3}. The test ring is fixed and has a torsional stiffness K_{rtu} whereas the reaction ring is free and has a torsional stiffness K_{rru}. The sun gears of both planetary gear sets are connected through a common shaft which has a torsional stiffness K_s. The carriers of both planetary gear sets are connected to each others through a hollow shaft which has a torsional stiffness K_c.

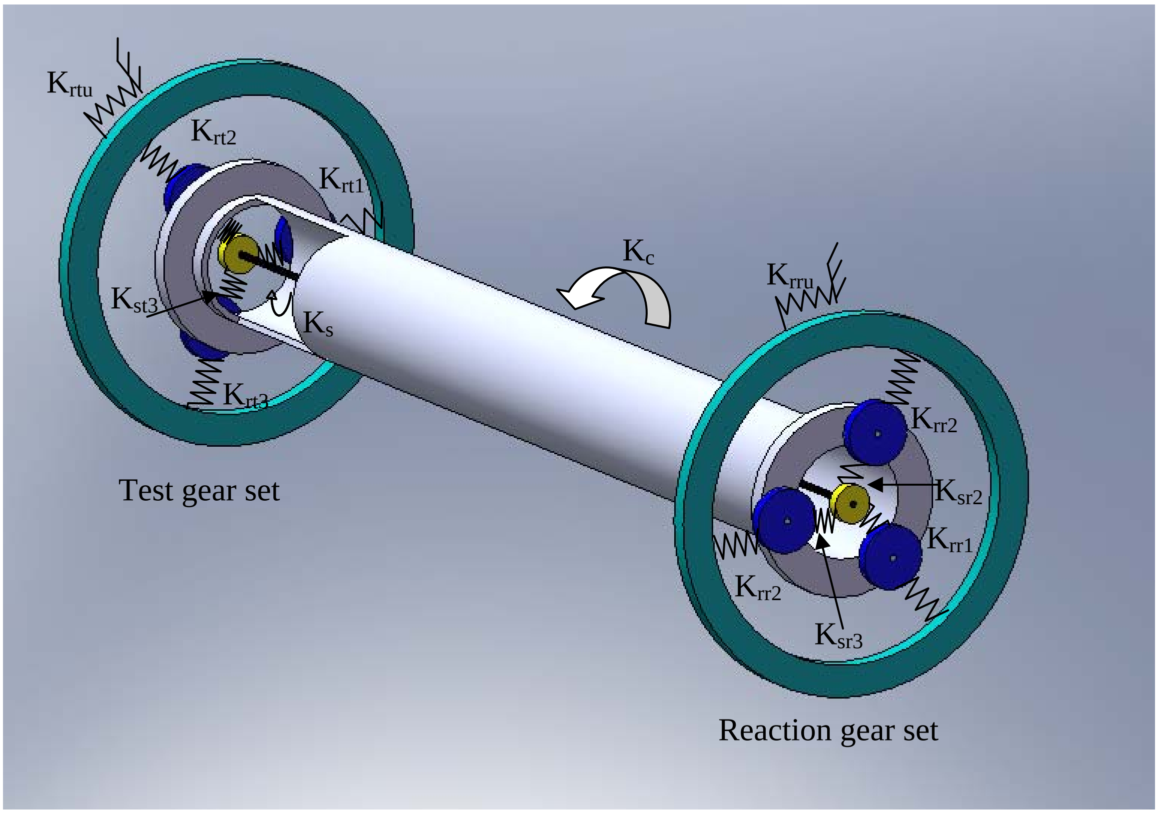

Fig.1: Model of planet gear

Only, rotational motions of the gear bodies are considered. The system's equation of motion for back to back planetary gear with 3 planets is:

$$M\ddot{q} + C\dot{q} + (K(t) + K_b)q = F(t) \quad (1)$$

Where the mass matrix is M . $K(t)$ is the stiffness matrix, K_b is the bearing matrix and $F(t)$ is the external torque vector applied on the system.

$K(t)$ can be divided into a mean stiffness matrix $\overline{K}$ and a time varying matrix $k(t)$:

$$K(t) = \overline{K} + k(t) \quad (2)$$

C is the proportional damping matrix expressed by :

$$C = \alpha M + \beta\overline{K} \quad (3)$$

Where α and β are two constants [17].

q is the degree of freedom vector expressed by:

$$q = \{u_{cr}, u_{rr}, u_{sr}, u_{1r}, u_{2r}, u_{3r}, u_{ct}, u_{rt}, u_{st}, u_{1t}, u_{2t}, u_{3t}\}^T \quad (4)$$

The rotational coordinates are $u_{rj} = r_{rj}\theta_{rj}$ for reaction gear set $u_{tj} = r_{tj}\theta_{tj}$ and for test gear set where j=c,r,s,1,2,3. θ_{rj} and θ_{tj} are the component rotation; r_{rj} and r_{tj} are the base radius for the sun, ring and planets and the radius of the circle passing through the planets centre for the carrier.

The resolution of the equation of motion is achieved using the implicit Newmark algorithm.

3. Description of the test bench

In order to validate numerical results, a test bench is developed at the department of structural and mechanical engineering of the University of Cantabria in Spain. It is composed of two identical planetary gear sets (Fig.2).

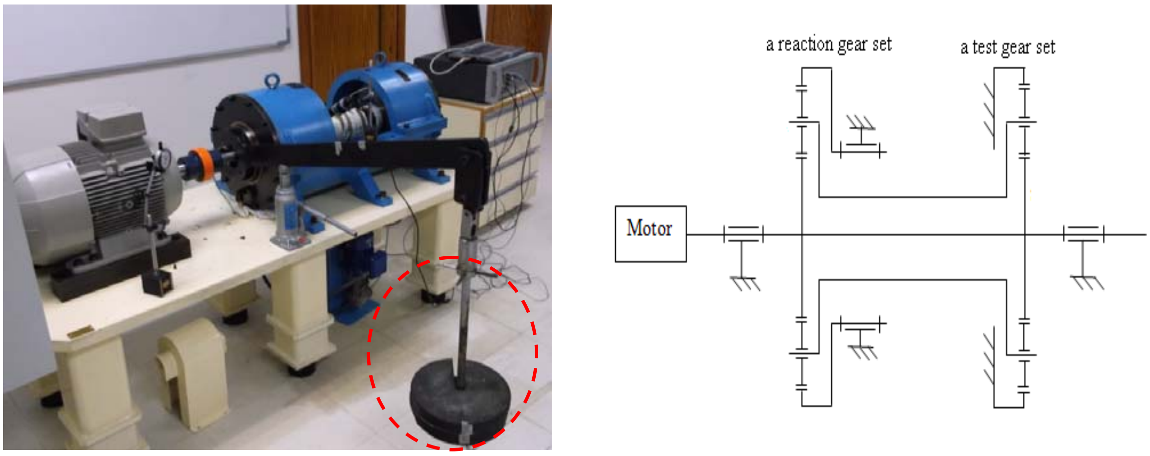

Fig.2: The test bench

The first planetary gear set is a test gear set and the second is a reaction gear set. The test gear set and the reaction gear set are connected back to back: the sun gears of both planetary gear sets are connected through a common shaft and the carriers of both planetary gear sets are connected to each others through a rigid hollow shaft (Fig.2).

An external torque is applied mechanically to the ring gear of the reaction gear set by adding mass on the arm while the ring gear of the test gear set is held stationary (Fig.2).

An electric motor is connected to the shaft of the sun gear to rotate both gear sets. Control of the electric motor is made by a frequency inverter “MICROMASTER 440” and the software “STARTER”.

Sensors used in this test bench are four tri axial accelerometers: two accelerometers are mounted in each ring (Fig.3). A tachometer measure the rotational speed of the carrier.

The signals are recorded by the acquisition system “LMS SCADAS” and the data is processed with the software “LMS Test.Lab” to obtain the acceleration spectra. Time histories were collected and averaged and later an autopower is used to obtain frequency spectra corresponding to each averaged time history.

(a) (b)

Fig.3: Tri axial accelerometers on the free ring (a) and the fix ring (b)

4. Numerical simulation and experimental validation

First of all, the dynamic behaviour of the model will be presented in stationary conditions. A time varying loading condition is than applied to the system. Besides, we will present the behaviour of the model during run up regime. In addition, we present a validation of numerical results with experimental results issued from the test ring.

4.1. Stationary conditions

The characteristics of the system are given in the table 1.

	Carrier	Ring	Sun	Planet
Teeth number	-	65	16	24
Moment of inertia (kgm²)	0.0021	0.697	0.0003	0.002
Base diameter (mm)	57.55	249.38	61.38	92.08

Table 1: Characteristics of the test bench

Three planets are considered for each planetary gear. The planets are positioned at angles and ψ_{nj} (n=1, 2, 3 and j=r, t) within the carrier where ψ_{nj} is measured relatively to the rotating basis vector.

Equally-spaced planets are considered for the reaction gear set $(0, \frac{2\pi}{3}, \frac{4\pi}{3})$ and for the test gear set $(\frac{\pi}{3}, \pi, \frac{5\pi}{3})$. Sequentially phased gear meshes ($\frac{Z_r \psi_{nj}}{2\pi} \neq n$ and $\sum_{n=1}^{N} Z_r \psi_{nj} = m\pi$ where n and m are integer) are considered for both test and reaction gears.

Time varying gear mesh stiffness sun-planets and ring-planets are modelled as square functions.

The back to back planetary gears are excited by meshing process at frequency (f_m=320.7 Hz) and its harmonics and the force due to the rotation of carrier which has a period T_c=0.2 s and frequency f_c=4.93 Hz. In addition, an individual influence of each planet on the accelerometer will be assumed for a duration T_c/N (N=3: number of planets). So, when a planet i approach to the location of the accelerometer, its influence will increase for the first $T_c/2N$ time period, reaching its maximum when the planet n is at the location of the accelerometer and then diminishing to zero at the end of the next $T_c/2N$ time period. This will be followed by the planet n+1 which dominates the response of the accelerometer for the next T_c/N time period, and so on [11].

4.1.1. Unloaded planetary gear

First simulation is performed for a fixed speed (1500 rpm) and fixed external load (0 N.m on the free reaction ring). The same conditions are used for the test bench. Fig.8 shows acceleration on fixed ring issued from simulation and experience on one period of rotation of carrier (T_c=0.2 s).

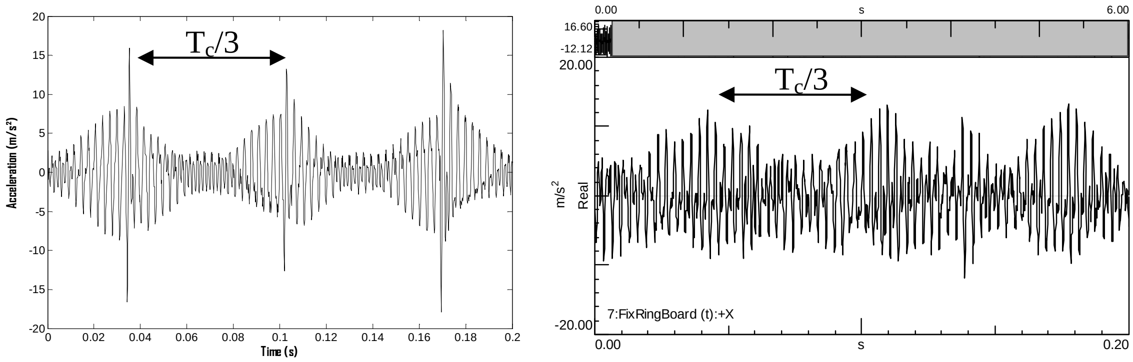

(a) (b)

Fig.4: Time response of the fix ring (a) theoretical and (b) experimental

In Fig.4, a clear amplitude modulation is observed as the signal repeats itself three times [11]. This amplitude modulation is explained by the modulation of the force due to rotation of carrier.

The spectra of dynamic component of the fix ring (Fig.5) shows that the back to back planetary gears is excited by meshing frequency (320.7 Hz) and its harmonics. In addition, sidebands appear on these spectra on the 3.n.f_c (n: integer) and m.f_c (m: integer).

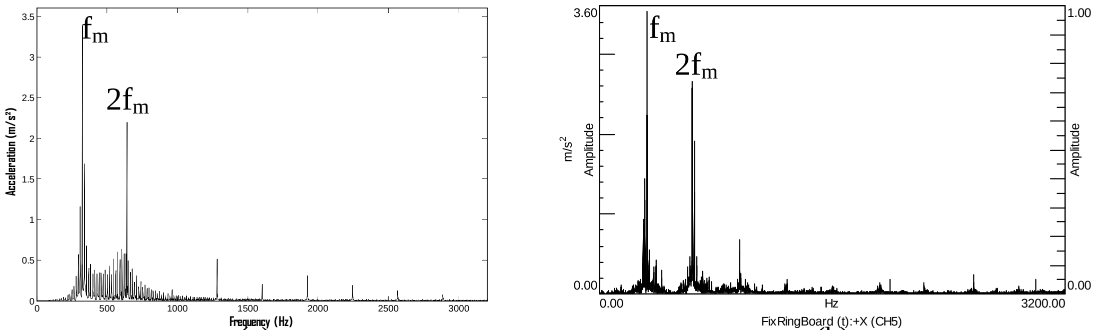

(a) (b)

Fig.5: Frequency response of the fix ring: Theoretical (a) and experimental (b)

The Fig.6 shows a zoom around f_m. It is clearly observed that the orders of all significant sidebands with sizable amplitudes are at f = n.N.f_c =nx3x4.9=nx14.7 Hz (*n*: integer and N=3: number of planets) in the vicinity of mesh order f_m=320.7 Hz. So, there are 4 harmonics with large amplitudes at frequencies of 296 Hz, 310 Hz, 326 Hz and 340 Hz, 370 Hz and 384 Hz.

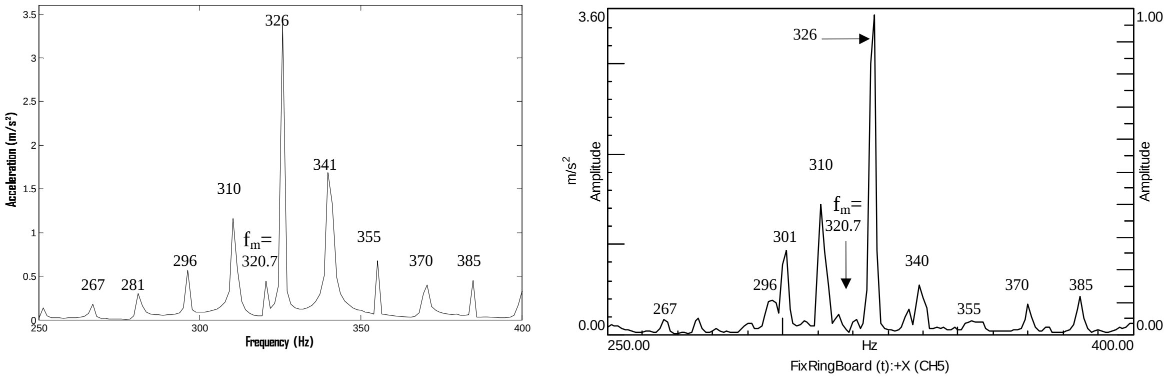

(a) (b)

Fig.6: Frequency response of the fix ring: Theoretical (a) and experimental (b)

Also, sidebands are mostly not symmetric about $f_m = 320.7\,Hz$. The harmonic order with the largest amplitude is the frequency f $_{max}$= n.N.f$_c$ =326 Hz that is the closest to f $_m$=320.7 Hz.

The order which is satisfying the condition is $\left| f_{\max} - f_m \right| \leq \frac{1}{2} N . f_c$

Meanwhile, when the harmonic of the meshing frequency is multiple of the number of planet (N=3), we have f $_{max}$= n.N.f$_m$ is the most important in amplitude. Figure 11 shows a zoom around the third harmonic of the mesh frequency 3f $_m$= 962 Hz.

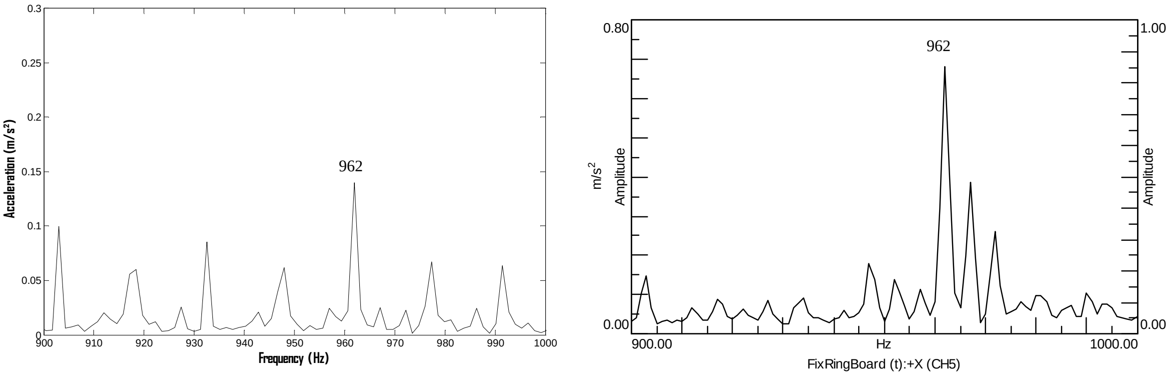

(a) (b)

Fig.7: Frequency response of the fix ring on the 3rd harmonic of meshing frequency (a) theoretical and (b) experimental

4.1.2. Loaded planetary gear

We make simulations and experiments with different loads: 100N.m, 300N.m, 500N.m, 700N.m and 900N.m. The dominant set of harmonics amplitude became 2f $_m$ (Fig.8).

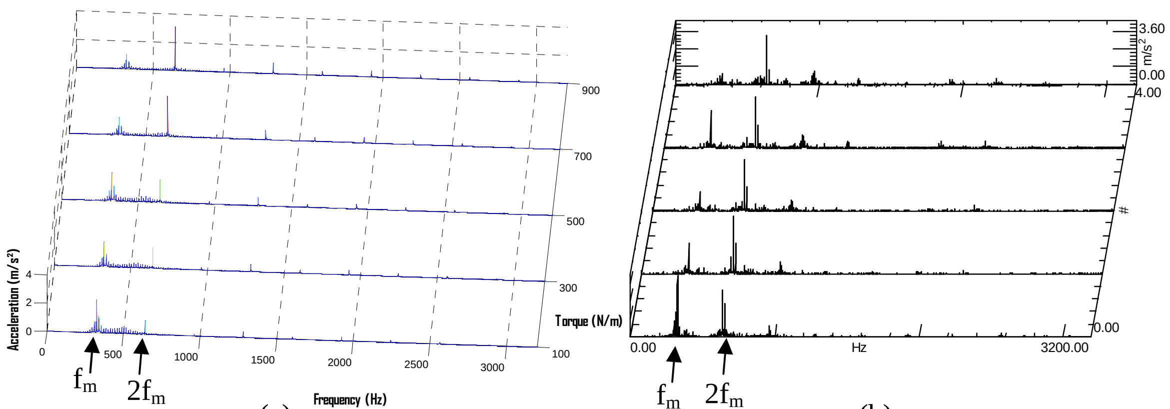

(a) (b)

Fig.8: Waterfall of frequency response of the fix ring with different load (a) theoretical and (b) experimental

Fig.8 shows that in each response, a dominant set of harmonics amplitude occurs in the neighbourhood of each tooth meshing frequencies. For the responses without load and with 100N.m of load, the dominant amplitude is in the fundamental tooth meshing frequency. As we increase the load, the dominant amplitude changes. For response with 900 N.m, the dominant amplitude is on the 2nd harmonic.

Mitchell [14] has recorded the vibration signature of gearbox of a marine steam turbine generator and reduced load from full to no load. He defined “intermediate frequencies” where an increase in amplitude was the earliest clear warning. The intermediate frequencies are produced by resonance of the gear elements excited by a repetitive variation in the tooth spacing or related to some other phenomena.

In our case, In addition to the variation of the tooth spacing, as we add mass, the external load, the torsional stiffness of the test ring K_{rtu} and the inertia of the test ring increase.

4.2. Non stationary conditions case

In the non stationary condition, the load or the speed of motor are variable in the time. For the variable speed, the dynamic behaviour of the system studied during the run up.

4.2.1. Variable load

We apply an external variable load on the free ring by adding and removing masses. The variation of the load is presented in Fig.9.

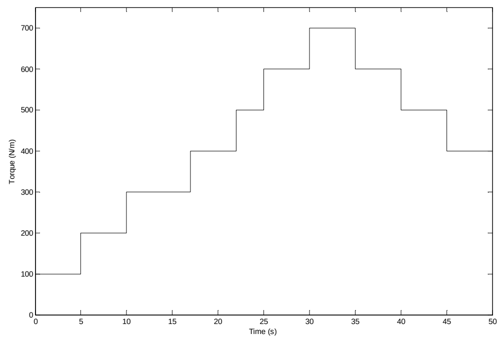

Fig.9: The external variable torque

The speed of motor is constant and is controlled by a frequency converter. The external load and the torsional stiffness of the test ring K_{rtu} are variable.

Fig.10 shows the time response of the fix ring. The acceleration of the fix ring decrease between 10s and 40s when the external torque increase. As the external torque increase, the torsional stiffness of the test ring K_{rtu} increase: this is why the system is more stable in this period.

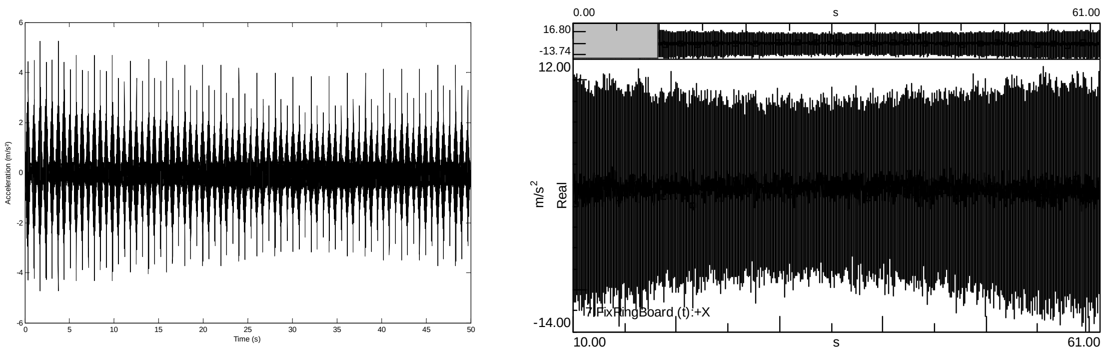

(a) (b)

Fig.10: Time response of the fix ring (a) theoretical and (b) experimental

Despite the system starts with the external torque 100N.m where the fundamental meshing frequency is the dominant (Fig.11). The frequency response of the fix ring shows that the 2nd harmonic of the meshing frequency (637 Hz) is the dominant.

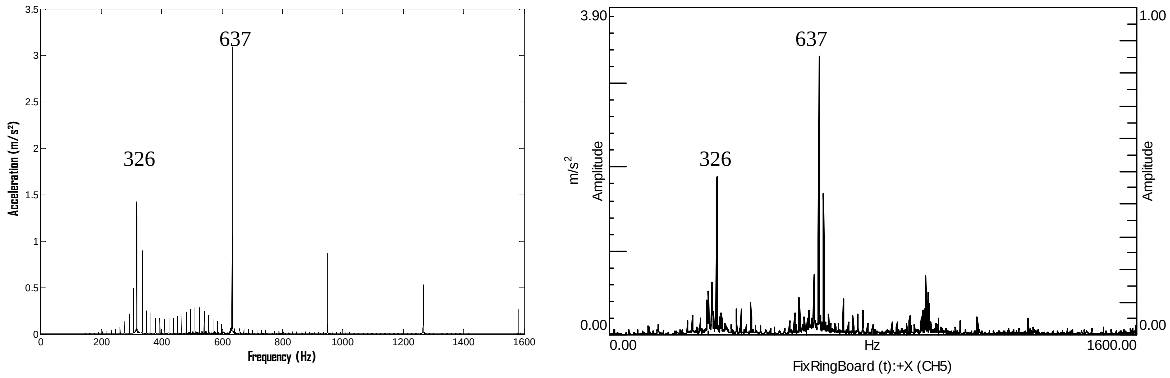

(a) (b)

Fig.11: Frequency response of the fix ring: Theoretical (a) and experimental (b)

With variable load, the dominate amplitude is on the 2nd harmonic of the mesh frequency which correspond to intermediate frequency as shown on fig.8.

4.2.2 Variable speed

The variation of speed is controlled by the frequency converter Micromaster 440. In this part, the dynamic behaviour of the system is presented during run up regime. Several systems are subjected to such repetitive regime during their exploitation. This regime is very critical since over loads can occur[18].

The frequency converter commands linearly the variation of the rotational speed of motor.

Fig.12 shows the experimental evolution of the motor's torque during run up.

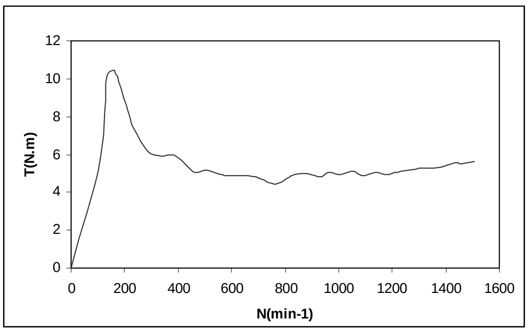

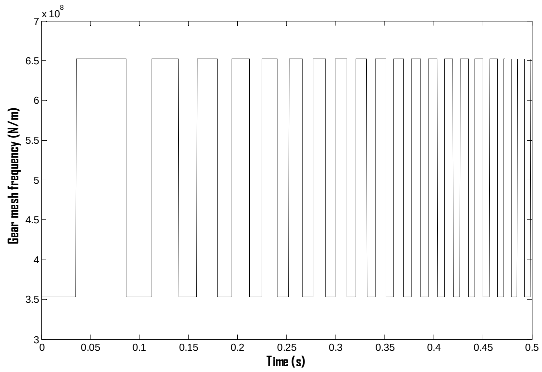

Fig.12: Torque of motor in the run up

Fig.13: Meshing stiffness in the run up

In the run up, the period of gear meshing decrease as we increase the speed (Fig. 13).

The run up can be very harmful for a gear transmission. It is very important to characterise the dynamic behaviour since naturals frequencies can be excited during this regime. To identify the eigen frequencies, an impact test is achieved. Fig.14 shows the FRF of the test ring.

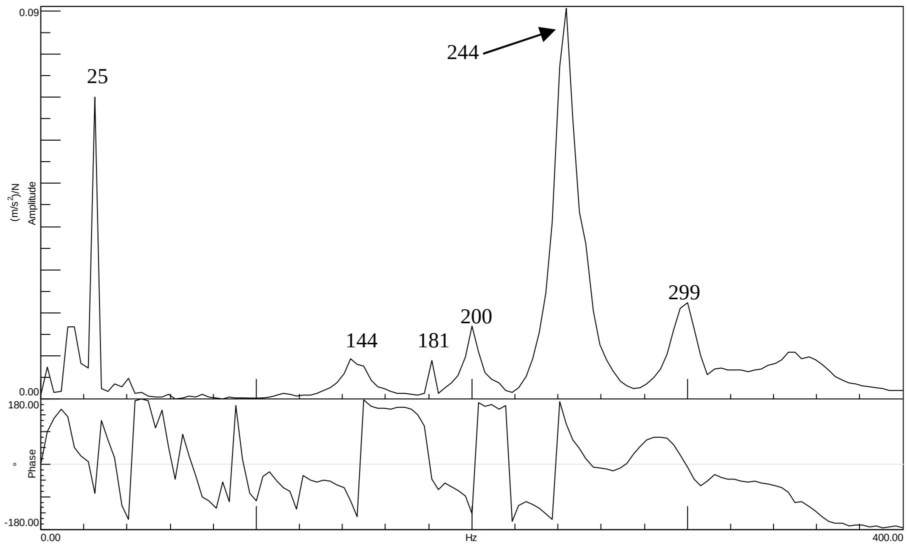

Fig.14: FRF of the fix ring

The largest amplitude of the resonant frequencies is on 244 Hz. In addition, the system is excited by the resonant frequencies 25 Hz, 144 Hz, 200 Hz and 299 Hz.

The time response of the acceleration on the fixed ring is shown in Fig.15. It is well observed that the vibration is increasing with respect to time. This is explained by the fact that during run up, the accelerating torque is increasing giving rise to increased vibration.

In addition, the amplitude of oscillation increases in the time.

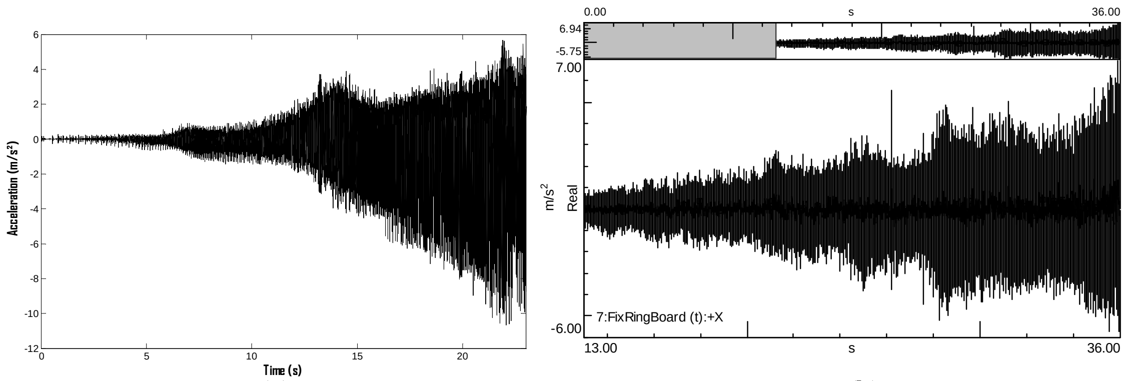

(a) (b)

Fig.15: Acceleration of the fix ring: (a) theoretical and (b) experimental

In the run up, the meshing frequency which excites the system is not constant. In order to describe the evolution of the frequency content during this phase, a time-frequency map is drawn based on Short Time Fourrier Transform (STFT).

Fig.16 shows STFT obtained from simulation and experience for acceleration on the test ring. It is clearly observed inclined lines showing the increase of the meshing frequency and its harmonics. In addition, vertical lines are observed and there are particular zones in which amplitude is more important which correspond some natural frequencies of the system.

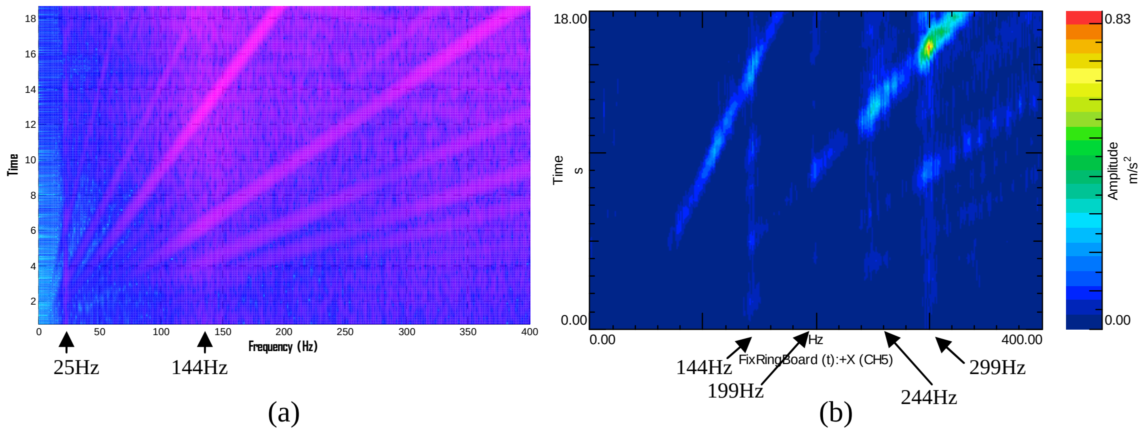

Fig.16: STFT of Colormap of the theoretical model (a) and the experimental result (b) of the

For simulation, two natural frequencies 25Hz and 144Hz are excited. For experimental results, we find that natural frequencies 144Hz, 199Hz, 244Hz and 299Hz are excited.

5. Conclusion

A back to back planetary gear dynamic model running under stationary and non stationary conditions is presented. A test rig of this transmission is also developed. Influence of run-up and time varying loading conditions were investigated. The main results obtained are:

- An external variable load applied on the free ring caused the amplification of the 2nd harmonic of the meshing frequency.
- Spectra of signals measured on accelerometers shows amplitude modulation induced by rotation of carrier. During rotation, the proximity or not of the planets from the accelerometers causes variability of the amplitude of measured vibrations.
- During run-up, accelerating torque is increasing giving rise to increased vibration with respect to time.
- Short time frequency analysis is used to characterize frequency content and identify the speed variation.
- Experimental results are in conformity with numerical issued form the developed model

Acknowledgements

This paper was financially supported by the Tunisian-Spanish Joint Project N° A1/037038/11.

References

[1] Randall R B. *A new method of modelling gear faults*, Journal of Mechanical Design, 1982, 104(2): 259–267

[2] Bartelmus W, Chaari F, Zimroz R, Haddar M. *Modelling of gearbox dynamics under time-varying non stationary load for distributed fault detection and diagnosis*, European Journal of Mechanics A/Solids, 2010, 29: 637–646

[3] Chaari F, Zimroz R., Bartelmus W.Fakhfakh T. and Haddar M. *Modelling of planetary gearbox for fault detection. Investigation on local damage size and time-varying load conditions influence to vibration response*, The Eighth International Conference on Condition Monitoring and Machinery Failure Prevention Technologies

[4] F. Chaari, R. Zimroz, W. Bartelmus, T. Fakhfakh, M. Haddar *Modelling of local damages in*

spur gears and effects on dynamics response in presence of varying load conditions

[5] Fakher Chaari, Mohamed Slim Abbes, Fernando Viadero Rueda, Alfonso Fernandez del Rincon, Mohamed Haddar *Analysis of planetary gear transmission in non-stationary operations*, Higher Education Press and Springer-Verlag Berlin Heidelberg 2013

[6] Woohyung Kim, Ji Yeong Lee, Jintai Chung *Dynamic analysis for a planetary gear with time-varying pressure angles and contact ratios*, 2011 Elsevier Ltd.

[7] Khabou MT, Bouchaala N, Chaari F, Fakhfakh T, Haddar M. *Study of a spur gear dynamic behavior in transient regime*, Mechanical Systems and Signal Processing, 2011, 25(8): 3089–3101

[8] Hidaka T, Terauchi Y (1976) *Dynamic behavior of planetary gear-1st Report, Load distribution in planetary gear.* Bulletin of the JSME 19:690-678

[9] Kahraman A (1999) *Static Load Sharing Characteristics of Transmission Planetary Gear Sets: Model and Experiment, Transmission and Driveline Systems Symposium.* SAE paper 01-1050

[10] Ligata H (2007) *Impact of system-level factors on planetary gear set behaviour,* Dissertation, The Ohio State University

[11] Inalpolat M, Kahraman A (2009) *A theoretical and experimental investigation of modulation sidebands of planetary gear sets.* J Soud Vib 323:677–696

[12] Jian Lin and Robert G. Parker, *Planetary gear parametric instability,* September 2007

[13] Jian Lin and Robert G. Parker, *Analytical characterisation of the unique properties of planetary gear free vibration*. July 1999.

[14] John S. Mitchell *Continuous monitoring systems for high speed gearing, Proceedings of the eleventh turbomachinery symposium*

[15] H.Ligata, A.Kahraman and A.Singh *An Experimental Study of the Influence of Manufacturing Errors on the Planetary Gear Stresses and Planet Load Sharing,* ASME, April 2008

[16] A.Singh A.Kahraman and H.Ligata, *Internal Gear Strains and Load Sharing in Planetary Transmissions – Model and experiments,* ASME and General motors, September 2007

[17] Dhatt G., Touzot G., *Une présentation de la méthode des éléments finis,* Paris, Editions Maloine S.A., 1984.

[18] R.J Drago. *The Effect of Start-Up Load Conditions on Gearbox Performance and Life Failure Analysis, with Supporting Case Study,* Gear Technology, June 2009.